n-Heptane As a Reducing Agent in the NO_x Removal over a Pt–Ba/Al_2O_3 NSR Catalyst

L. Righini,[†] L. Kubiak,[†] S. Morandi,[‡] L. Castoldi,[†] L. Lietti,*[,†] and P. Forzatti[†]

[†]Dipartimento di Energia, Laboratory of Catalysis and Catalytic Processes and NEMAS, Centre of Excellence, Politecnico di Milano, P.zza L. da Vinci 32, Milano, Milano, Italy

[‡]Dipartimento di Chimica and NIS Inter-Departmental Center, Università di Torino, Via P. Giuria 7, 10125 Torino, Torino, Italy

1. INTRODUCTION

LNTs (Lean NO_x Traps) and SCR (Selective Catalytic Reduction) technologies are employed to cope with the regulations (i.e., Euro and Tier standards) related to the emission of NO_x in the exhausts of diesel and lean-burn gasoline engines.[1−3] LNTs (also referred to as NSR, NO_x Storage-Reduction catalysts) represent a promising solution for light duty vehicles. These catalytic systems have been introduced in the 1990s by Toyota and comprise precious metals (Pt, Rh, Pd), storage components (alkali or alkaline-earth metal oxides, like Ba or K), and promoters (like Ce, Zr), supported on a high surface area material, typically γ-Al_2O_3.[1,4,5] Their working conditions alternate long lean phases of a few minutes, occurring under the normal operation of the engine, with short rich phases of a few seconds. During the lean phase NO_x are adsorbed on the storage compound; upon the periodic short excursion to rich conditions the stored NO_x are reduced to N_2 and other byproducts, like NH_3 and N_2O.

Several studies analyzed the NO_x adsorption and reduction (regeneration) processes.[6−12] It has been reported that regeneration is a Pt catalyzed process, possibly evolving through two steps. Initially the stored NO_x diffuse on the surface toward Pt sites, resulting in a NO release or formation of NO related intermediates; these species are then reduced to N_2 and byproducts.[6,9] The reactivity of reductants like H_2,[13−15] CO,[16−19] and short chain hydrocarbons (HCs)[20−27] (e.g., C_3H_6 and C_3H_8) has been extensively investigated in the literature.

On the other hand, investigations using long chain hydrocarbons, that are more representative of diesel fuels, are more scarce.[28]

For this reason, the aim of this study is to explore systematically the catalytic behavior and the pathway involved in the reduction of stored NO_x when a long chain HC, like *n*-heptane, is used. This molecule has been selected since it has a cetane number comparable with European diesel fuel. Accordingly, the reaction between the selected hydrocarbon and the adsorbed NO_x has been investigated over a PtBa/Al_2O_3 model NSR catalyst through transient techniques by performing NO_x storage-reduction cycles under isothermal conditions and temperature-programmed experiments in a flow microreactor system. *In situ* FT-IR spectroscopy has also been employed to analyze the nature of the adsorbed species involved in the reactions. For comparison purposes, the reactivity of *n*-heptane with gaseous NO has also been studied.

Received: June 18, 2014
Revised: August 13, 2014
Published: August 15, 2014

Experiments have been carried out both in the absence and in the presence of water to analyze the role of such species in the reduction process. The role of oxygen, which may be present in small amounts during the regeneration process, has also been investigated, and results are shown in the following.

2. EXPERIMENTAL SECTION

2.1. Materials. This investigation has been carried out over a model homemade Pt−Ba/Al_2O_3 (1/20/100 w/w) catalyst. Metals have been incorporated by an incipient wetness impregnation method over a commercial alumina sample (Versal 250 from UOP). First the support has been calcined at 700 °C for 10 h in order to obtain an γ-Al_2O_3 phase. Subsequently the support was impregnated with an aqueous solution of dinitrodiammine platinum (Strem Chemicals, 5% Pt in ammonium hydroxide) and then with a solution of barium acetate (Aldrich, 99%), in line with Toyota patents procedures.[29,30] Drying at 80 °C overnight and calcination in air at 500 °C for 5 h followed each impregnation step.[31]

The obtained catalyst has a specific surface area of 160 m^2 g^{-1} (BET method), an average pore diameter of 17 nm, and a pore volume of 0.72 cm^3 g^{-1}, determined using a Micromeritics TriStar 3000 instrument. Pt dispersion of 52% was measured by hydrogen chemisorption at 0 °C (TPD/R/O 1100 Thermo Fischer Instrument). The sample has been characterized by XRD diffraction using a Philips PW 1050/70 diffractometer; peaks related to microcrystalline γ-Al_2O_3, orthorhombic and monoclinic $BaCO_3$ (traces), and small ones possibly related to Pt^0 have been observed.[32]

2.2. Apparatus and Procedures. The catalyst has been tested in a flow microreactor system. Catalyst powder (60 mg, 70−100 μm) has been loaded in a quartz tube microreactor (7 mm I.D.), and a flow of 100 N cm^3/min was set to obtain a GHSV of 10^5 h^{-1}. The effluent stream was analyzed online by mass spectrometry (QMS 200, Pfeiffer Vacuum) and FTIR analysis (MKS 2030 FTIR MultiGas analyzer).[33]

n-Heptane has been fed by flowing a He current through a saturator, held at 0 °C (with a mixture of ice and water). The other reactants have been obtained by mixing gases from calibrated cylinders.

Isothermal (ICSC, Isothermal Concentration Step Change) and temperature-programmed experiments (TPSR, Temperature-Programmed Surface Reaction, and TPR, Temperature-Programmed Reaction) have been performed.

ICSC experiments have been carried out at 250, 300, and 350 °C. In a typical run, NO_x storage (lean phase) has been accomplished by stepwise admission of 500 ppm of NO in 5% v/v O_2 to the reactor at the selected temperature until steady-state conditions have been reached. After a He purge, a rectangular step feed of *n*-C_7H_{16} (∼900 ppm in He) has been admitted to the reactor (rich phase). A 4-way valve has been used to accomplish step changes in the inlet reactant concentration, and Ar was used as internal tracer. Typically three cycles have been performed, and the third cycle will be discussed in the following. After the last adsorption/reduction cycle, a cleaning treatment with 2000 ppm of H_2 and subsequently with 2% v/v of H_2O and 3% v/v of O_2 have been carried out at the selected temperature to remove residual adsorbed species. N-balances, estimated as difference between the amounts of stored NO_x species during the adsorption phases, and evolved N-containing species during the rich phases and final cleaning treatments, generally closed within ∼10%.

In a typical TPSR experiment, NO_x have been adsorbed like during ICSC experiments (i.e., with a flow of 500 ppm of NO + 5% v/v of O_2 in He) at 350 °C.[7,10,34] After a He purge at 350 °C to remove weakly adsorbed species, the catalyst has been cooled to 50 °C. Then ∼900 ppm of *n*-C_7H_{16} have been admitted to the reactor, and the catalyst temperature has been linearly increased up to 400 °C with a rate of 10 °C/min. The experiment has been followed by cleaning treatments with H_2 first (2000 ppm) and then with H_2O (2% v/v) + O_2 (3% v/v) at 400 °C.

When the effect of water or oxygen has been studied during TPSR experiments, 2% v/v of H_2O or 0.1/3% v/v of O_2 have been fed during the reduction phase.

Finally, the reactivity of the *n*-heptane in the Steam Reforming reaction, combustion with O_2 and reduction of gaseous NO has also been investigated with TPR tests. In a typical experiment, the catalyst has been exposed to a mixture of reactants (see Table 1) under temperature programming from 50 to 400 °C (heating rate 10 °C/min). Final cleaning treatments with H_2 and a mixture of H_2O and O_2 have been performed to remove residual surface species, if any.

Table 1. TPR Run Experimental Conditions (Species and Concentrations, ppm) from 50 to 400°C, 10 °C/min over a Pt−Ba/Al_2O_3 Catalyst

TPR run	C_7H_{16}	NO	O_2	H_2O	CO_2
C_7H_{16} + O_2	900	–	1000	–	–
C_7H_{16} + H_2O	900	–	–	20000	–
C_7H_{16} + H_2O + CO_2	900	–	–	20000	10000
C_7H_{16} + NO	900	1000	–	–	–
C_7H_{16} + NO + O_2	900	1000	1000/30000	–	–
C_7H_{16} + NO + H_2O	900	1000	–	20000	–

The catalytic tests have been performed over a conditioned sample, i.e. after a few NSR cycles carried out at 350 °C by feeding 1000 ppm of NO in 3% v/v O_2 during the lean phase and H_2 (2000 ppm) as reducing agent in the rich phase. Conditioning lasted until reproducible catalytic performances have been attained.

In situ absorption/transmission FT-IR spectra were carried out on a PerkinElmer FT-IR System 2000 spectrophotometer equipped with a Hg−Cd−Te cryo-detector, working in the range of wavenumbers 7200−580 cm^{-1} at a resolution of 2 cm^{-1} (number of scans ∼20). The catalyst powder samples were compressed in self-supporting discs (10 mg cm^{-2}) and placed in a commercial heated stainless steel cell (Aabspec) allowing *in situ* thermal treatments under vacuum or controlled atmosphere and the simultaneous registration of spectra at temperatures up to 600 °C.

Before the IR experiments, the samples were fully conditioned, i.e. submitted to *i)* outgassing at 500 °C for 30 min, *ii)* three storage-reduction cycles consisting of NO_2 adsorption at 350 °C followed by reduction in H_2 at 350 °C, and *iii)* outgassing at 500 °C and cooling down to the requested temperature.

FT-IR experiments were performed both in isothermal conditions and at increasing temperature in the range 100−400 °C (steps of 50 °C, 10 min at each temperature) to be compared with experiments performed in the microreactor unit. However, differently from catalytic tests, IR measurements were performed in static conditions with mixture of gases, whose relative pressures are specified in the figures. When the

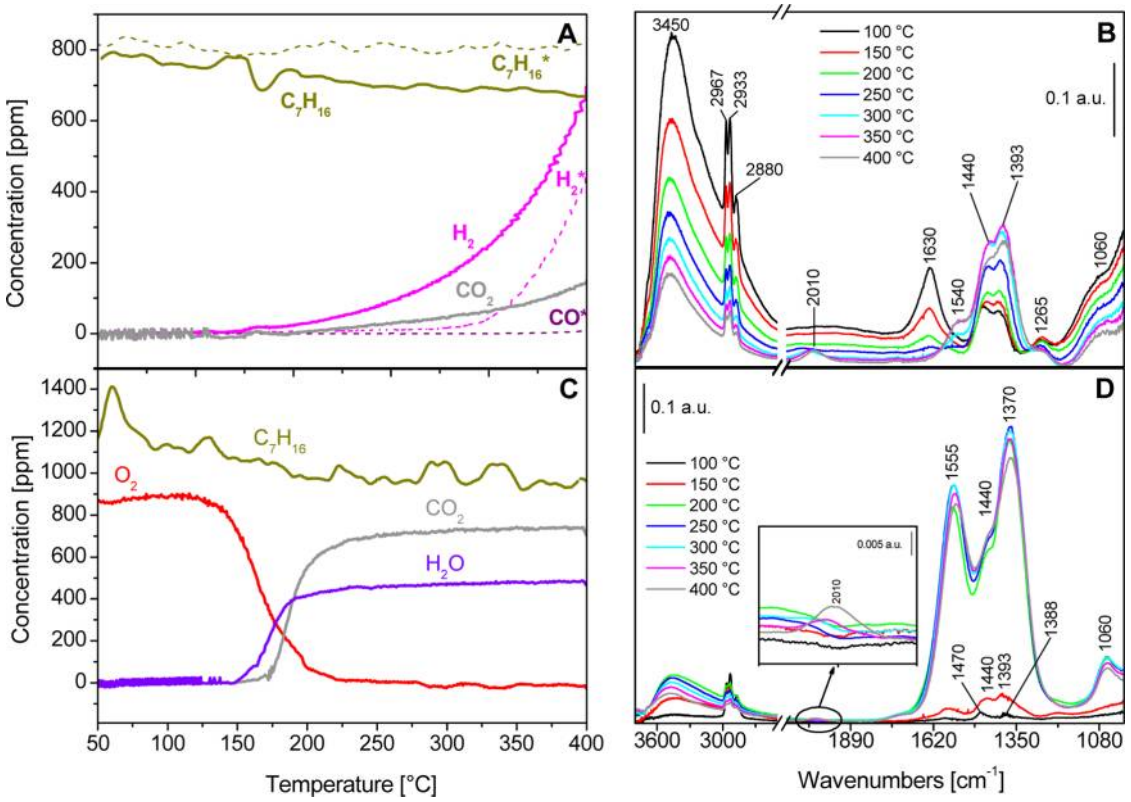

Figure 1. TPR experiments over Pt−Ba/Al_2O_3 from 50 to 400 °C, 10 °C/min. A) *n*-heptane (900 ppm) + H_2O (2% v/v) (*n*-heptane +2% v/v of H_2O + 1% v/v CO_2 as dashed lines) and C) *n*-heptane (900 ppm) + O_2 (1000 ppm). FTIR spectra of Pt−Ba/Al_2O_3 upon admission of *n*-heptane (2 mbar) at increasing temperature: B) with H_2O (10 mbar) and D) with O_2 (2 mbar).

reduction of stored NO_x has to be investigated, the NO_x storage has been carried out at 350 °C by admitting NO_2 (p_{NO2} = 5 mbar) up to catalyst saturation (ca. 20 min) followed by outgassing at 350 °C and cooling down to the requested temperature.

3. RESULTS AND DISCUSSION

3.1. Reactivity of *n*-Heptane with H_2O and O_2. The reaction of *n*-heptane with H_2O and O_2 has been preliminarily investigated by performing TPR experiments and FT-IR analysis.

Figure 1A shows the results of the *n*-C_7H_{16}-TPR run carried out with 2% v/v H_2O. Above 200 °C evolution of H_2 and CO_2 is detected (solid lines in Figure 1A), due to the occurrence of the Steam Reforming (SR) and Water−Gas Shift (WGS) reactions, according to the stoichiometry of reactions 1 + 2 = 3:

$$C_7H_{16} + 7H_2O \rightarrow 15H_2 + 7CO \quad (1)$$

$$CO + H_2O \rightarrow H_2 + CO_2 \quad (2)$$

$$C_7H_{16} + 14H_2O \rightarrow 22H_2 + 7CO_2 \quad (3)$$

The poor CO concentration detected in the gas phase is due to the occurrence of the WGS reaction 2, approaching chemical equilibrium under the investigated experimental conditions at 400 °C (K_{eq} = 11; K_{sp}/K_{eq} ~1).

Concerning *n*-heptane, its consumption is hardly observable due to its low conversion even at the highest investigated temperature.

When the reaction is carried out in the presence of 1% v/v of CO_2 (dashed lines of Figure 1A), the threshold of SR reaction is delayed, being H_2 observed at higher temperatures, above 300 °C. Then its concentration increases, and a maximum of roughly 450 ppm has been observed at 400 °C, along with almost 10 ppm of CO. Also under these conditions at 400 °C the WGS reaction is close to equilibrium, but in this case small amounts of CO are detected due to the high CO_2 concentration shifting reaction 2 from right to left.

In Figure 1B the FT-IR spectra obtained upon admission of the *n*-heptane/H_2O (1:5) mixture over PtBa/Al_2O_3 at increasing temperature are shown. Already in the spectrum obtained at 100 °C many vibrational bands are present, associated with H-bonded surface hydroxyls (ν(OH) at 3450 cm^{-1}), adsorbed H_2O molecules ($\nu_{asym.}(H_2O)$ and $\delta(H_2O)$ at 3450 and 1630 cm^{-1}, respectively), adsorbed C_7H_{16} molecules ($\nu_{asym.}(CH_3)$, $\nu_{sym.}(CH_3)$, $\nu_{asym.}(CH_2)$ and $\nu_{sym.}(CH_2)$ at 2967, 2880, 2933, and 2870 cm^{-1}, respectively), surface ionic carbonates (1440 and 1393 cm^{-1}, deriving by the splitting of the corresponding double degenerate $\nu_{asym.}(CO_3)$ mode of free carbonates and $\nu_{sym.}(CO_3)$ mode at 1060 cm^{-1}[135]), and surface bicarbonates (ν(C−OH) at 1265 cm^{-1}[136]). The shape of the spectra at frequency lower than 1200 cm^{-1} is related to the bending modes of surface hydroxyls.

On increasing the temperature, bands related to adsorbed water and heptane decrease in intensity, as expected. It is reasonable that at high temperatures the bands at 2967, 2933, and 2880 cm^{-1} might be also related to C−H stretching modes of C_xH_y fragments deriving from heptane cracking. Unfortunately, C−H stretching modes of these fragments are not distinguishable from that of heptane. Also the bands related to bicarbonates decrease with temperature due to the surface dehydration. Otherwise, bands related to ionic carbonates increase up to 350 °C. Starting from 300 °C a band related to

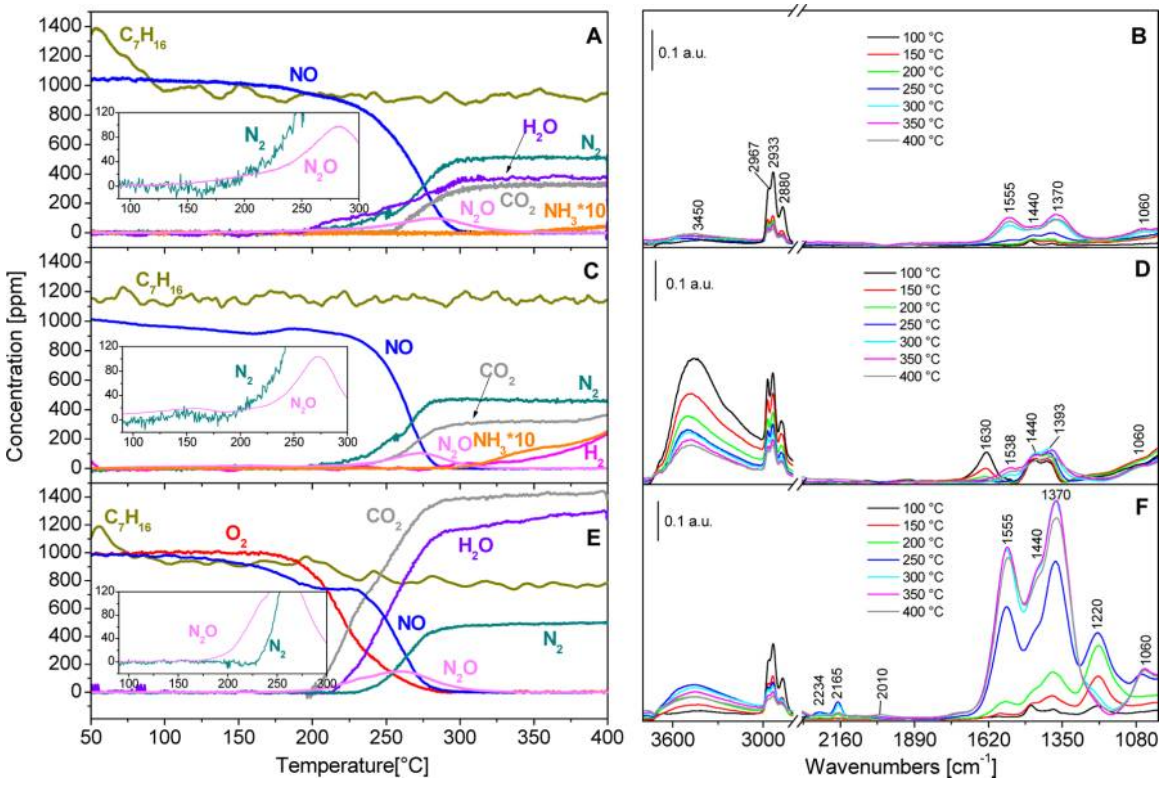

Figure 2. TPR experiments over Pt−Ba/Al_2O_3 from 50 to 400 °C, 10 °C/min. A) NO (1000 ppm) + *n*-heptane (900 ppm); C) NO (1000 ppm) + *n*-heptane (900 ppm) + H_2O (2% v/v); E) NO (1000 ppm) + *n*-heptane (900 ppm) + O_2 (1000 ppm). FT-IR spectra of NO reduction with *n*-heptane at increasing temperature: B) NO (2 mbar) + *n*-heptane (2 mbar); D) NO (2 mbar) + *n*-heptane (2 mbar) + H_2O (2); 2 mbar); F) NO (2 mbar) + *n*-heptane (2 mbar) + O_2 (2 mbar).

bidentate carbonates (ν(C═O) at 1540 cm^{-1}[136,37]) appears, and simultaneously bands related to ionic carbonates decrease in intensity. This is related to the effect of surface dehydroxylation that converts ionic carbonates into bidentate ones,[35] as already observed for nitrates and reported in ref 38.

Moreover, at 300 °C, a band related to CO adsorbed on Pt sites at 2010 cm^{-1} is also visible.[39] The formation of such Pt carbonyls is in line with the occurrence of the Steam Reforming reaction, although no detectable amounts of CO have been observed at the reactor outlet. According to previous data[40] the WGS reaction is catalyzed by Pt; however, formation of Pt carbonyls is observed during FTIR analysis at slightly higher temperatures if compared to H_2/CO_2 evolution in microreactor experiments likely due to their very low concentration at such low temperatures. Figures 1C and D show the results obtained in the reaction *n*-C_7H_{16} with 1000 ppm of O_2 ((*n*-C_7H_{16}+O_2)-TPR run). As shown in Figure 1C, oxygen consumption starts near 150 °C, and it is complete near 225 °C, due to the occurrence of the combustion reaction 4 with formation of H_2O and of CO_2 (this last species with a delay probably ascribed to the adsorption on the catalyst surface as $BaCO_3$).

$$C_7H_{16} + 11O_2 \rightarrow 8H_2O + 7CO_2 \quad (4)$$

Traces of CO (ca. 5 ppm, not displayed in Figure 1C) have also been detected, possibly suggesting the occurrence of the *n*-C_7H_{16} partial oxidation reaction as well (in view of the low O_2 concentration in the feed).

At the beginning of the heating ramp at 50 °C a *n*-heptane peak is seen, due to its desorption from the surface (this peak was not observed in the experiment of Figure 1A possibly due to the presence of water competing with *n*-heptane for adsorption over the surface). Also in this case, the consumption of *n*-heptane is not clearly observable.

When the reaction is carried out with higher O_2 concentration (3% v/v, data not reported), complete consumption of the hydrocarbon is observed, but no effects have been observed on the onset of the combustion reaction. CO_2 and H_2O have been seen as reaction products.

In Figure 1D FT-IR spectra of a PtBa/Al_2O_3 catalyst upon admission of the *n*-heptane/O_2 (1:1) mixture are shown. At 100 °C bands related to adsorbed *n*-heptane molecules are mainly present; in this case it is possible to observe also the bands related to $\delta_{asym.}(CH_3)$ and $\delta_{sym.}(CH_3)$ at 1470 and 1388 cm^{-1}, respectively, along with the bands related to the corresponding stretching modes in the range 2800−3000 cm^{-1}. At 150 °C formation of ionic (1440, 1393, and 1060 cm^{-1}) and bidentate (1555, 1370, and 1060 cm^{-1}) carbonates is well evident along with the formation of H-bonded hydroxyls (3450 cm^{-1}). Carbonates and OH groups derive from CO_2 and H_2O adsorption, respectively, confirming the threshold temperature of the combustion reaction. At 200 °C carbonate bands suddenly increase along with that of OH groups. On increasing temperature, on one hand hydroxyl band decreases, as expected, because of their low thermal stability; on the other hand the intensities of carbonate peaks show a short-growing, pointing out that the major part of oxygen is consumed already at 200 °C, in agreement with the gas phase analysis.

Starting from 350 °C, a weak band at 2010 cm^{-1}, related to CO adsorbed on Pt sites, has been also observed (see inset in Figure 1D), in line with the very small amounts of CO detected at the reactor outlet due to the occurrence of the *n*-C_7H_{16} partial oxidation reaction.

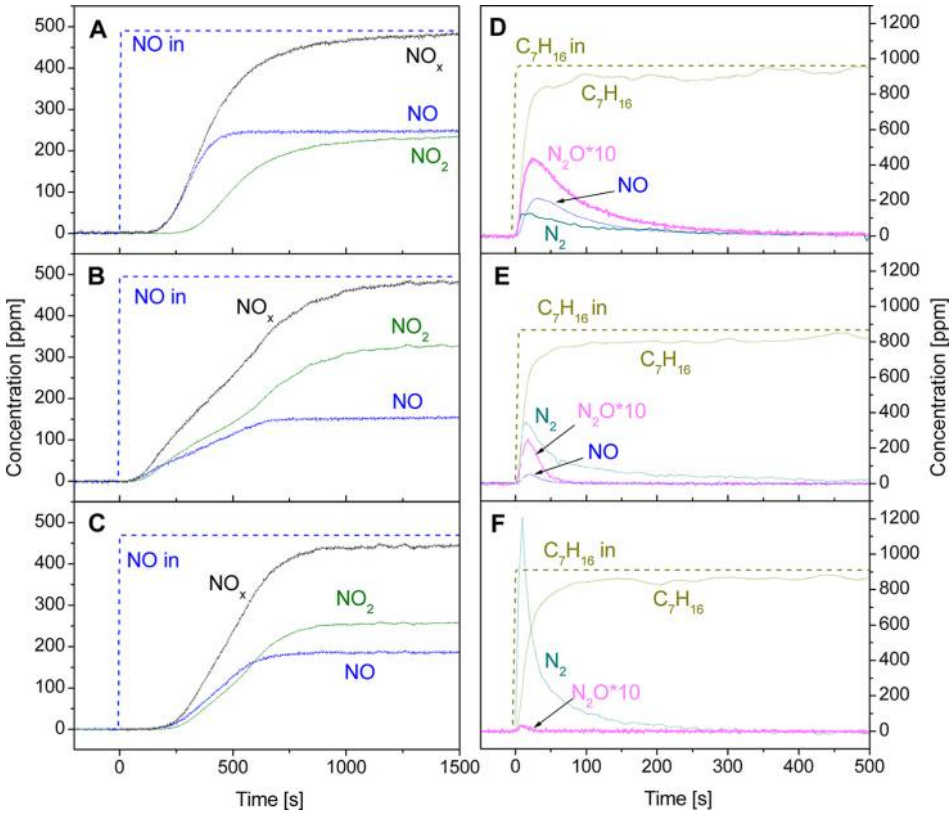

Figure 3. Isothermal Step Concentration experiments respectively at 250 °C (A–D), 300 °C (B–E), and 350 °C (C–F) over the Pt–Ba/Al_2O_3 catalyst; adsorption phase: NO 500 ppm + O_2 5%v/v in He flow; reduction phase: *n*-heptane 900 ppm in He flow.

3.2. Reactivity of *n*-Heptane with Gaseous NO. Figure 2A shows the results obtained during the (*n*-C_7H_{16}+NO)-TPR experiment. The reaction is monitored near 200 °C with a small evolution of N_2 and of N_2O. The N_2O concentration shows a maximum near 280 °C, whereas above 300 °C, upon complete NO consumption, the reaction is highly selective to N_2, whose concentration at steady state agrees with the stoichiometry of reaction 5. From 350 °C trace amounts of NH_3 are also detected (~7 ppm).

$$C_7H_{16} + 22NO \rightarrow 11N_2 + 7CO_2 + 8H_2O \quad (5)$$

According to the stoichiometry of reaction 5, NO reduction by *n*-heptane is accompanied by H_2O and CO_2 formation (CO_2 evolution delayed possibly due to its adsorption on Ba sites, as shown by FT-IR analysis reported in Figure 2B). Notably, the small *n*-heptane consumption expected according to the stoichiometry of reaction 5 (less than 50 ppm) explains why it is not visible in the *n*-C_7H_{16} concentration trace.

This experiment clearly shows that the *n*-heptane is able to reduce selectively gaseous NO, although the reaction is monitored at relatively high temperatures if compared to other reductants like H_2 and CO.[23,33]

The reaction is selective to N_2, although significant amounts of N_2O have been observed at low temperatures. As suggested in previous studies,[12,41,42] this might be related to a nonefficient reduction of the oxygen-covered Pt sites at low temperatures. This prevents the NO dissociation thus promoting the formation of N_2O instead of N_2. This point will be discussed in the following.

The corresponding surface analysis is reported in Figure 2B. In the spectrum recorded at 100 °C it is possible to observe only the bands related to adsorbed *n*-heptane molecules in the region 3000–2800 cm^{-1} and at 1470 and 1388 cm^{-1}. Starting from 150 °C, carbonates (bands at 1555, 1440, 1370, and 1060 cm^{-1}) and hydroxyls (band at 3450 cm^{-1}) are formed, and their amounts increase with temperature, in agreement with TPR measurement. No other surface species have been detected, including NCO species.

At variance, formation of NCO species has been reported in the literature upon reaction of NO_x with a short chain hydrocarbon (like C_3H_6) over a $PtBa/Al_2O_3$ catalyst.[23,43,44] According to Abdulhamid et al.,[23] the detection of isocyanate species during the reduction of stored NO_x with C_3H_6 and with CO suggests that the regeneration of NO_x proceeds via the same reaction pathways for these two reducing agents. DiGiulio et al.[27] argued that NCO formation during the reduction of stored NO_x with propylene could be ascribed to the presence of CO, whose evolution may be explained by the oxidation of C_3H_6. In fact it is well-known that isocyanate species can be easily obtained upon reduction of NO with CO.[16]

As a matter of fact, no CO formation has been observed in our case. This possibly explains why we do not collect evidence for NCO formation during the reduction of NO with *n*-heptane under our experimental conditions.

However, the formation of other intermediate surface species (e.g., oxygenated compounds like aldehydes, ketones, and alkoxides formed upon oxidation of *n*-heptane to CO_2) cannot be excluded in view of the overlapping with the carbonates related bands.

Figure 2C shows the results of the (*n*-C_7H_{16}+NO)-TPR run carried out in the presence of H_2O. The results are similar to those obtained under dry conditions (Figure 2A), with formation of N_2O and of N_2 starting from 200 °C. Notably, with respect to the run carried out in dry conditions, the full

conversion of NO is however attained at slightly lower temperatures under wet conditions (280 °C vs 300 °C). This is likely due to the presence of H_2 produced by SR + WGS reactions; being H_2 a more efficient reductant than *n*-heptane, an enhancement of the reduction process is observed. This further modifies the selectivity of the process, favoring the N_2 selectivity near 300 °C and NH_3 formation at high temperatures.

Accordingly the presence of water does not significantly affect the NO reduction process by *n*-heptane, although, due to H_2 production via SR+WGS, a reaction pathway involving H_2 formation followed by NO reduction, according to reaction 6, can operate as well.

$$2H_2 + 2NO \rightarrow N_2 + 2H_2O \quad (6)$$

However, the H_2 produced via SR+WGS under wet conditions (see Figure 1A) cannot quantitatively explain the amounts of N_2 produced. This indicates that even in the presence of water, NO cannot be uniquely reduced by H_2 produced via the SR + WGS reactions.

The IR spectra collected during the exposure of the sample to the *n*-C_7H_{16} + NO + H_2O mixture are shown in Figure 2D. The evolution of carbonates is observed already at 100 °C (bands at 1440, 1393, and 1060 cm^{-1}), at temperature lower than that observed in dry conditions. In this case, the OH spectral region is dominated by the band of H-bonded hydroxyls of both molecular water (at low temperature, see also band at 1630 cm^{-1} related to the $\delta(H_2O)$) and surface OH groups. As already mentioned, the shape of the spectra at frequency lower than 1200 cm^{-1} is related to the bending modes of surface hydroxyls. It is worth noting that in this case ionic carbonates (bands at 1440 and 1393 cm^{-1}) are mainly formed, being bidentate carbonates (band at 1538 cm^{-1}) evident only at the highest temperatures. Otherwise, in dry conditions (Figure 3B) bidentate carbonates (bands at 1555 and 1370 cm^{-1}) are mainly present. This is related to the effect of surface hydroxylation that converts bidentate carbonates into ionic ones.[35,38]

The reduction of gaseous NO by *n*-C_7H_{16} has been performed in the presence of O_2 as well (1000 ppm), and the results are shown in Figure 2E. The temperature onset for NO consumption is observed at slightly lower temperatures if compared to the O_2-free runs, and it is seen below 150 °C. However, no correspondent evolution of N-containing products has been observed, suggesting the adsorption of NO on the catalyst surface. This is confirmed by the FT-IR measurement reported below. N_2O appears from 170 °C, evolving with a maximum, along with N_2 which is seen above 230 °C. At variance with the previous cases (Figures 2A and 2C), in the presence of oxygen N_2O formation is favored at low temperatures, evolving prior to N_2 (see insert in the Figure). Finally, O_2 consumption starts from 175 °C and is complete above 300 °C.

The FT-IR spectra (Figure 2F) show that in the presence of O_2, NO is adsorbed on the catalyst surface already at 100 °C in the form of nitrites (band at 1220 cm^{-1} related to $\nu_{asym.}(NO_2)$ mode).[34] This accounts for the NO consumption observed at low temperatures in Figure 2E. The nitrite band reaches the maximum intensity at 250 °C, being eroded at higher temperature, possibly involved in the reaction with heptane and/or transformed into nitrates.[34] However, the presence of nitrates is not clearly visible due to the overlapping of their bands with those of carbonates at 1555, 1440, 1370, and 1060 cm^{-1}. As a matter of fact, due to *n*-heptane combustion with O_2, the maximum intensity reached by carbonate bands is roughly seven times higher than that reached in the experiences reported in Figure 2B and 2D. For the same reason, also the maximum intensity reached by the hydroxyl band at 3450 cm^{-1} is higher with respect to that reached in dry conditions (Figure 2B).

In the spectra of Figure 2F the presence of two bands at 2234 and 2165 cm^{-1}, related to linearly bonded NCO and ionic NCO species, respectively, is also observed.[16,38] Since these species have not been observed only during the (NO+*n*-C_7H_{16})-TPR (Figure 2B), it is likely that they do not come from the direct NO reduction with the *n*-heptane. However, formation of such species is typically observed in the presence of CO,[16,18,19,23,27] and the formation of this species may be originated here by *n*-heptane partial combustion and/or Steam Reforming with water produced *in situ* by *n*-heptane combustion. Indeed the formation of CO has not been detected in the gas phase, but it is pointed out by the band at 2010 cm^{-1} related to Pt-CO species. As a matter of fact, formation of NCO species during the reduction of NO with C_3H_6 in the presence of oxygen has been explained by Bisaiji et al.[45] by the occurrence of HCs partial oxidation reactions.

The presence of 3% v/v O_2 in the *n*-C_7H_{16}+NO reaction system (data here not reported) does not affect the temperature thresholds for the reactions but changes the selectivities, leading to a significant evolution of N_2O (up to 268 ppm) along with N_2, whose formation shows a maximum near 250 °C. At higher temperatures N_2 production decreases and NO is oxidized to NO_2. Hence *n*-heptane is able to reduce NO_x under strong lean conditions but in a rather narrow temperature windows, as typically observed for the HC-SCR catalytic systems.

3.3. Reactivity of *n*-Heptane with Stored NO_x Species.

The reactivity of *n*-heptane with stored NO_x species has been investigated both at constant temperatures (ICSC experiments) and under temperature programming (TPSR runs).

The results of ICSC runs carried out at 250, 300, and 350 °C are shown in Figure 3A–F, where the third adsorption/reduction cycle has been reported (only N-containing products are shown).

Figure 3A reports the data collected at 250 °C during the lean phase. Upon NO admission to the reactor at $t = 0$, a NO breakthrough is observed, and then its concentration increases up to a constant value. NO_2 is also detected due to the occurrence of NO oxidation reaction. The adsorption of NO_x is accompanied by the evolution of CO_2 (not shown in the figure) due to the displacement of Ba carbonates upon NO_x storage. By increasing the temperature the amount of stored NO_x, evaluated at 1500 s (Figure 3A, B and C), increases showing a maximum at 300 °C (0.319 mmol/g_{cat}). At the end of the storage nitrates are present on the surface, as pointed out elsewhere.[34]

Reduction of stored NO_x has been carried out at the same temperature of the adsorption. At 250 °C upon the addition of ca. 900 ppm of *n*-heptane (Figure 3D), a peak of NO and of N_2 is observed, along with minor amounts of N_2O. The selectivity to N_2 is near 50%, while those to NO and N_2O are near 35 and 15%, respectively. Besides, only 50% of the initially stored NO_x are removed during reduction. These adsorbed species could be removed after the final cleaning treatment with H_2 (see the Experimental Section) that shows the evolution of N_2 and of NH_3. By taking into account these evolved species the overall

nitrogen mass balance related to the cycles is satisfied within ±10%.

Upon increasing the temperature, the reduction process becomes faster and more selective: the peaks related to the reduction products are sharper and formation of N_2 is favored, so that at 350 °C the N_2 selectivity is almost 100%. At higher temperatures the efficiency of the reduction of the stored NO_x is also increased and is near 60% on the third cycle.

Notably, the reduction process is initially very fast but then becomes slow, and not all the stored NO_x species could be removed. It is speculated that when the hydrocarbon is activated on Pt, it breaks down into C_xH_y fragments, and some residual carbon species may block Pt sites, preventing the complete reduction of the stored NO_x. Poisoning effects have been invoked also by other authors to explain the low reduction efficiency of CO and C_3H_6 in the reduction of stored NO_x.[28,44]

Figure 4 displays the evolution of surface species upon reduction of the stored NO_x with *n*-heptane at 350 °C as a function of time. In this case the stored NO_x have been obtained at 350 °C starting from NO_2. However, it has been shown that the same species (nitrates) are obtained at saturation and at 350 °C upon adsorption of either NO/O_2 or NO_2.[46]

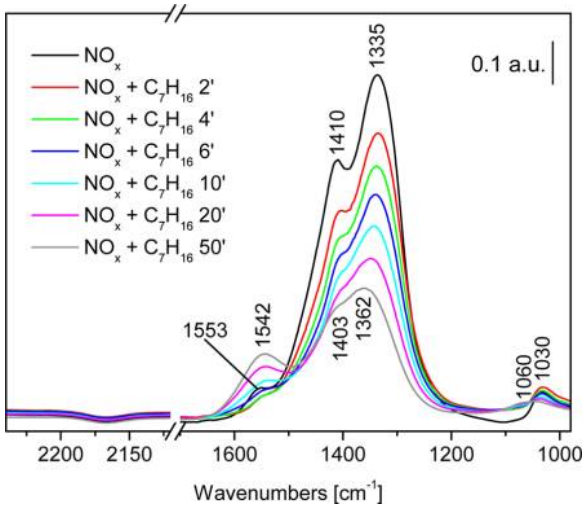

Figure 4. FT-IR spectra of NO_x reduction with 2 mbar of *n*-heptane at 350 °C at increasing time over the $Pt-Ba/Al_2O_3$ catalyst. Black line: spectrum recorded after admission of NO_2 (5 mbar) at 350 °C up to saturation and subsequent evacuation at 350 °C.

The spectrum of the stored species (black line) was recorded after NO_2 outgassing at 350 °C and shows bands related to ionic nitrates ($\nu_{asym.}(NO_3)$ mode split in two peaks at 1410 and 1335 cm^{-1}; $\nu_{sym.}(NO_3)$ mode at 1030 cm^{-1}) and minor amounts of bidentate nitrates ($\nu(N{=}O)$ mode at 1553 cm^{-1}).[7,34] Upon admission of *n*-heptane, nitrates are reduced, and the related bands gradually decrease in intensity. After 10 min, the increase on increasing time of the band at 1542 cm^{-1} related to the $\nu(C{=}O)$ mode of bidentate carbonates indicates that the reduction reaction (with production of CO_2 and thus of carbonates) is occurring. After 50 min also the absorption related to the $\nu_{sym.}(C{-}O)$ mode of carbonates at 1060 cm^{-1} is evident. In agreement with ICSC results, after 50 min the reduction is not complete, and residual nitrates are present on the surface, as evidenced by a weak peak at 1030 cm^{-1} and by the shape of spectrum in the range 1500–1300 cm^{-1}. As a matter of fact, the spectral feature in this region with two maxima at 1403 and 1362 cm^{-1} is generated by the superimposition of carbonate and nitrate bands.

It is worth noting that in this run no formation of NCO species has been observed, at variance with what was reported by DiGiulio et al.[27] These authors pointed out the formation of isocyanate species upon reduction of stored NO_x by C_3H_6 over $Pt-Ba/Al_2O_3$ and $Rh-Ba/Al_2O_3$ catalysts both at 250 and 350 °C. However, different operating conditions (and a different reductant) have been adopted in this study. In particular, CO formation has been observed in their FT-IR analysis, explained by an *in situ* generation from C_3H_6, and this may explain the observed differences considering the role of CO in isocyanate formation discussed above.

The influence of H_2O on the reduction process between 250 and 350 °C has been addressed as well (data here not reported). The reduction is slightly slower (the peaks related to the formation of reduction products are less sharp), and ammonia is seen among the reaction products. As already discussed about Figure 2C, formation of ammonia is possibly due to the reduction of NO_x by H_2 produced via SR and WGS reactions. Notably, even for the experiments carried out in a wet stream, the final cleaning treatment with H_2 has to be applied to obtain the complete removal of the stored NO_x.

The reactivity of *n*-heptane toward stored NO_x has also been investigated by temperature programming experiments (TPSR) and FT-IR analysis.

Figure 5A shows the results of TPSR experiments carried out under dry conditions, performed after the storage of NO in the presence of O_2 at 350 °C (0.18 $mmol/g_{cat}$ of adsorbed NO_x). The reaction threshold is near 220–250 °C, where NO (few ppm) and N_2 evolution is observed. At 370 °C NH_3 is also detected in trace amounts. By neglecting the small amounts of NO and NH_3, the reduction of stored nitrates is in line with the stoichiometry of the following overall reaction:

$$5C_7H_{16} + 22Ba(NO_3)_2 \rightarrow 22N_2 + 22BaO + 35CO_2 + 40H_2O \quad (7)$$

Notably, the onset for the reduction reaction is well below that of the thermal decomposition of nitrates (near 350 °C)[32] but above the temperature onset for the *n*-heptane/NO reaction (Figure 2A). This indicates that the regeneration does not involve the thermal decomposition of the stored nitrates as initial step. Notably, the reduction of the stored NO_x is a Pt catalyzed processes, since it does not occur over a Pt free sample (data not published), as also seen in the case of other reductants.[13]

FT-IR spectra recorded upon *n*-C_7H_{16} contact at different temperatures after NO_x adsorption at 350 °C (Figure 5B) show the decrease of the nitrate bands (ionic nitrates at 1426, 1327 and 1030 cm^{-1}; bidentate nitrates at 1553 cm^{-1}) above 200–250 °C; reduction ends at 400 °C when nitrate bands are no longer present, while bands related to bidentate carbonates at 1542, 1376, and 1060 cm^{-1}, ionic carbonates at 1440 cm^{-1} and hydroxyl groups at 3450 cm^{-1} (not shown in the figure), derived from the reduction, are observed. As already mentioned, nitrate and carbonate bands are superimposed in the region 1600–1200 cm^{-1}, and it is possible to evaluate the temperature at which the complete removing of nitrates occurs from the nitrate band at 1030 cm^{-1}. Finally, no bands assignable to isocyanates are observed (see previous section).

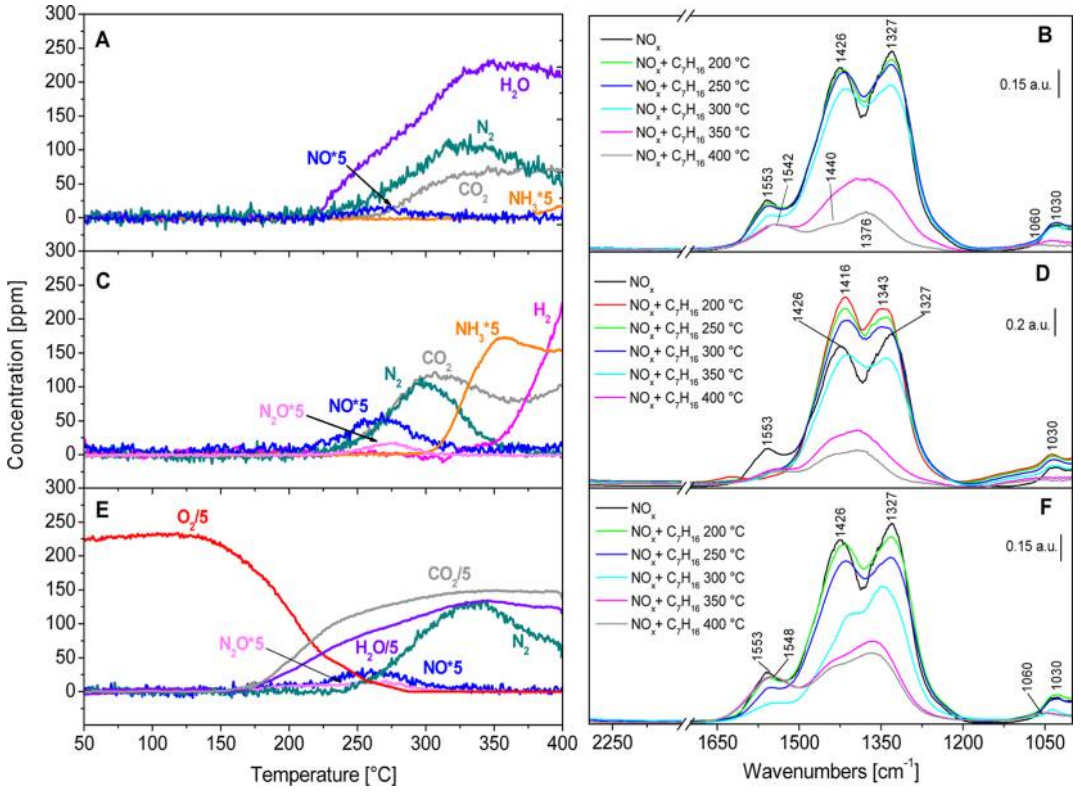

Figure 5. Reduction of stored NO_x species from 40 to 400 °C, 10 °C/min. A) *n*-heptane (900 ppm); C) *n*-heptane (900 ppm) + H_2O (2% v/v); E) *n*-heptane (900 ppm) + O_2 (1000 ppm). FT-IR spectra recorded during the reduction of nitrates (black line: spectrum recorded after admission of NO_2 (5 mbar) at 350 °C up to saturation and subsequent evacuation at 350 °C): B) *n*-heptane (2 mbar); D) *n*-heptane (2 mbar) + H_2O (10 mbar); F) *n*-heptane (2 mbar) + O_2 (2 mbar).

The reduction of nitrates with *n*-C_7H_{16} has also been investigated in the presence of H_2O, and results are shown in Figure 5C. If compared to the run performed under dry conditions, some differences can be appreciated: (i) NO formation is slightly enhanced among the reaction products and traces amounts of N_2O can be also detected; (ii) the maximum in the N_2 concentration is reached slightly at lower temperatures; (iii) NH_3 is formed in higher amounts. Moreover, H_2 is detected from 300 °C, and its concentration sharply increases above 350 °C.

A comparison of the H_2 evolution trace of Figure 5C with that obtained in the absence of adsorbed NO_x (Figure 1A) suggests the involvement of H_2 in the regeneration process, i.e. H_2 formed via the SR + WGS reactions reacts with stored nitrates. This may also explain the shape of the CO_2 concentration trace: the initial evolution of CO_2 likely originates from the reduction of stored nitrates, while the evolution at high temperatures could be ascribed to the occurrence of the SR and WGS reactions. However, the amounts of H_2 formed via SR+WGS (Figure 1A) are well below the quantities of N_2 produced according to the stoichiometry of reaction 8, i.e. the reduction reaction of stored nitrates with H_2:

$$5H_2 + Ba(NO_3)_2 \rightarrow N_2 + Ba(OH)_2 + 4H_2O \qquad (8)$$

This indicates that even in the presence of water H_2 does not quantitatively account for the whole N_2 production and further suggests that the reduction pathway via SR and WGS reactions is not the unique pathway for the reduction of stored NO_x, in line with findings of Al-Harbi et al.[28]

FT-IR data of the reduction of the stored nitrates by *n*-heptane in the presence of water are reported in Figure 5D. In this case, initially the interaction with water converts bidentate nitrates (erosion of band at 1553 cm^{-1}) into ionic ones (increase of bands at 1426 and 1323 cm^{-1} that shift to 1416 and 1343 cm^{-1}, respectively). In fact the dissociative chemisorption of water takes place in a competitive way on surface sites on which bidentate nitrates are formed; the dislocated nitrates remain on surface portions with sites able to form the ionic species, as extensively discussed by some of us in ref 38. The conversion of bidentate nitrates into ionic ones operated by surface hydroxylation does not allow identification of the onset temperature of the reduction by *n*-heptane. From the evaluation of the nitrate band at 1030 cm^{-1}, it is possible to state that the reduction ends already at 350 °C. At the end of the reduction carbonates and hydroxyl groups (not shown in the figure) are observed. Also in this case, no bands assignable to isocyanate species are detected.

When the reduction of the stored nitrates by *n*-heptane has been carried out in the presence of O_2 (1000 ppm, Figure 5E), results similar to those collected in the absence of oxygen has been obtained. A slightly higher reduction onset temperature is seen, along with a higher formation of NO and of N_2O. NH_3 formation is negligible. By comparing this result with that obtained during the (*n*-C_7H_{16}+O_2)-TPR (Figure 1C), it appears that the thresholds of the combustion reaction (monitored through the consumption of O_2 and the evolution of CO_2 and H_2O) are similar, but in the absence of stored nitrates (i.e., in the case of the TPR run, Figure 1C) the combustion reaction proceeds faster. This might suggest an inhibiting effect of the stored nitrates over the *n*-heptane

combustion reaction. An inhibition effect of stored NO_x over the C_3H_6 combustion reaction has also been pointed out by Anderson et al.[47] over a $PtBa/Al_2O_3$ catalyst and by Oh et al.[48,49] over Pt/Al_2O_3 systems.

Figure 5F shows the surface FT-IR analysis obtained during the reaction of *n*-heptane with the stored nitrates in the presence of oxygen. In agreement with TPR results, no relevant changes have been observed with respect to the measurement performed without oxygen in dry conditions (see Figure 5B), except higher amounts of carbonates at the end of the reduction, as expected.

4. MECHANISTIC ASPECTS INVOLVED IN THE REDUCTION OF STORED NO_X BY HYDROCARBONS

In this work mechanistic aspects involved in the regeneration of stored NO_x and gaseous NO with *n*-C_7H_{16} have been investigated by performing isothermal and temperature programming experiments, coupled with the analysis of surface species performed by FT-IR spectroscopy. It appears that the *n*-heptane is an effective reductant of both gaseous NO and stored NO_x at temperatures above 200 and 250 °C, respectively. Therefore, gaseous NO is more easily reduced than stored NO_x. In both cases, the reduction leads to the selective formation of N_2 above 300 °C, but significant amounts of N_2O are also formed at lower temperatures. The parallel FT-IR analysis pointed out the presence of a number of adsorbed species including *n*-C_7H_{16} (and possibly C_xH_y fragments), nitrites and nitrates, carbonates and bicarbonates, CO, and isocyanate species, whose concentration depends on the experimental conditions, i.e. temperature, presence/absence of H_2O, gas-phase NO, and oxygen.

Mechanistic aspects involved in the reduction of NO and stored NO_x with hydrocarbons are still under debate. Many studies refer to the HC-SCR concept,[49−58] that may be relevant for LNTs as well. According to Burch et al.,[50−54] the reduction of gaseous NO in an oxygen rich environment may proceed over PGM catalysts via NO dissociation to give N(ads) and O(ads). Adsorbed oxygen atoms are removed by the reductant, whereas formation of N_2 occurs via coupling of N-adatoms. The role of the reductant is hence to keep Pt in a reduced state (i.e., to provide Pt empty sites), on which NO may dissociate. The reaction may also involve the formation of organo-nitro-type species intermediates and/or adsorbed NO_x species (e.g., nitrates),[50−54] although their role is not precisely known. In fact, formation of CN, NCO, and RNO_2 species has been reported, although it is difficult to say whether these species are involved as intermediates or simply act as spectators.[50]

Epling and co-workers[28] investigated the reduction with hydrocarbons (propylene, *n*-dodecane and *m*-xylene) of NO_x stored over a $Pt-Ba/Al_2O_3$ LNT catalyst. These authors reported that three possible pathways may be involved in the reduction of stored NO_x. One route implies in the activation of the hydrocarbon molecule, through adsorption on Pt sites, followed by the fragmentation of the molecule into reactive subspecies. Organic chains of different length, saturated or unsaturated, have been suggested as possible subspecies.[6,59] These reactive fragments interact with gaseous NO/stored NO_x, giving rise to organic nitro- and isocyanate intermediate species, which are eventually transformed into N_2. In line with this route FT-IR analysis showed the presence of NCO species over a $Pt-Ba/Al_2O_3$ catalyst,[23,26,27,44] both in the presence and in the absence of O_2.[60] Nevertheless, it is not completely clear whether NCO species are spectators or reactive intermediates in the N_2 formation.[27] The second pathway involves at first the reduction (or cleaning) of Pt sites by the reductant, which drives the NO dissociation, as proposed for a PGM catalysts.[50] In this respect, the mechanism likely involves the release of NO before the dissociation step. The O-adatoms formed upon NO dissociation participate in the oxidation of the hydrocarbon, while N-adatoms are converted into N_2. Finally, according to the third route, under wet streams the hydrocarbon is reformed to H_2 and CO,[28] which are effective reductants for the stored NO_x, according to the pathways already discussed in the literature for these species.[14,17]

Based on the data previously reported, it is suggested that the reduction of the stored NO_x by *n*-C_7H_{16} in He proceeds according to the pathway sketched in Scheme 1.

Scheme 1. Sketch of Stored NO_x Reduction Mechanism with *n*-Heptane over a $Pt-Ba/Al_2O_3$ Catalyst

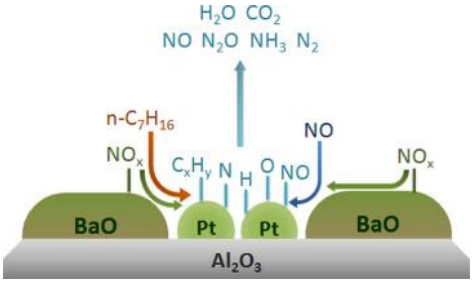

Upon admission of *n*-heptane at sufficiently high temperatures, O-adspecies are scavenged from Pt sites, and this leads to the activation/destabilization of the NO_x stored nearby Pt. Eventually the stored NO_x lead to the release of NO in the gas phase and/or result in the formation of NO-related intermediates adsorbed over Pt. NO_x species adsorbed far from the Pt spill to the reduced noble metal before decomposition. The released NO (or the NO-related intermediates) dissociate over reduced Pt sites into N- and O-adatoms: the O-adatoms are scavenged by the hydrocarbon fragments leading to CO_x and H_2O, whereas N-adatoms may recombine with undissociated NO molecules, with other N-adatoms, or with H-adspecies to give N_2O, N_2, and NH_3, respectively.[42,61] According to this picture, and in line with FTIR data, nitrocyano compounds like isocyanate are not formed to a significant extent, and it is likely that they are not involved in the reduction pathway. Instead a pool of adsorbed species is present on Pt sites (N-, O-, and H-adatoms along with C_xH_y fragments and undissociated NO molecules), whose concentration depends on the operating conditions and that are involved in coupling reactions leading to the reaction products.

According to the pathway suggested above, the reduction of the stored NO_x is initiated by the reduction of the noble metal. Following previous XPS data,[32] under oxidizing conditions (i.e., at the end of the adsorption phase) Pt sites are oxidized, while during the reduction phase free metallic sites (reduced Pt) are obtained. In this respect, *n*-heptane shows a rather poor reactivity since the reduction of Pt sites and hence the reaction (both with stored NO_x and with gaseous NO) is observed at higher temperatures if compared to other reductants like H_2 and, to a lower extent, CO.[33] On the other hand TPSR experiments with *n*-heptane and propylene show comparable onset temperatures.[20] The reduction of Pt drives the spillover of the stored NO_x and the following release. Once Pt is

reduced, the rate of NO_x spillover/release also affects the process, being gaseous NO reduced faster than the stored NO_x.

During the reduction, the selectivity of the products depends on the Pt oxidation state: reduced Pt sites will favor NO decomposition, followed by N−N coupling leading to N_2, while partially and/or totally O-covered Pt sites lead to the release of unreacted NO and of N_2O, whose formation requires the participation of undissociated NO molecules.[42] This explains the selectivity changes observed e.g. during ICSC experiments (Figure 3), where evolution of NO and N_2O is seen at low temperatures (due to the presence of O-covered Pt sites) and almost complete selectivity to N_2 is attained at high temperatures, when Pt is fully reduced. Similar effects are observable during TPR and TPSR experiments, where the evolution of small but non-negligible amounts of N_2O (and also of NO in the case of TPSR experiments) have been observed at low temperatures.

In line with the role of the Pt reduction state on the selectivity of the reaction, the presence of O_2 in the feed keeps Pt in a slightly oxidized state (i.e., covered by O-adatoms) particularly at low temperatures, and this favors N_2O formation. It is worth noting that a much higher N_2O formation has been observed during TPR runs if compared to TPSR experiments in view of the much higher concentration in the gas-phase.

Notably, during ICSC experiments at constant temperature the reduction process is not able to fully reduce the stored NO_x. This is likely due to the formation of C_xH_y adspecies or other carbonaceous fragments formed upon decomposition of the *n*-heptane molecule and blocking the Pt sites.

In view of the suggested picture, the regeneration process is built on a complex sequence of steps: at first stored NO_x species are released as NO or NO-related intermediates, which are converted to different products according to the oxidation state of Pt. In this regard, it is likely that both the reduction of Pt sites and the release of NO from the stored NO_x affects the rate of the process. Indeed by applying reductants with increasing reducing power (i.e., H_2 > CO > *n*-C_7H_{16}) the onset temperature for the reduction of stored NO_x decreases,[33] indicating the key role played by the reductant. However, the observation that in all cases gaseous NO is more readily reduced if compared to the stored NO_x species (compare the onset temperatures of TPR vs TPSR data) further indicates that the rate of NO release from the stored species affects the overall reduction process.

When the reduction has been carried out under wet streams, no significant differences have been observed with respect to the dry feed, in spite of the fact that under wet conditions the hydrocarbon is involved in the SR and WGS reactions, as previously shown (Figure 1A and 1B). These reactions lead to the formation of H_2 and CO_2, being CO (produced via the SR reaction) readily converted into CO_2. H_2 produced according to these routes participates in the reduction of stored NO_x; nevertheless, the data here presented indicate that the reduction via SR route is not able to account quantitatively for the formation of N_2, as discussed above in the case of TPR and TPSR data. In fact NO_x are reduced even in the absence of water according to the pathway previously depicted (Scheme 1), indicating that the occurrence of the SR route is not essential for the NO_x reduction. In any case under wet conditions the produced H_2 participates in the reduction of stored NO_x and also leads to the formation of NH_3 whose evolution is indeed greatly enhanced in the presence of H_2.

At variance with our data, other authors reported the formation of NCO species upon reduction of gaseous and/or stored NO_x with hydrocarbons (e.g., C_3H_6).[23,27,44] Therefore, the intermediacy of isocyanate species in the reduction process has been suggested. These differences may be ascribed to the small CO formation in our experiments, that in turn affects the presence of NCO, being the formation of this species related to the presence of CO.[18] As a matter of fact, in the reduction with C_3H_6 of NO_x stored over $Pt/BaO/Al_2O_3$ and $Rh/BaO/Al_2O_3$ catalysts, Di Giulio et al.[27] reported the formation of NCO species but showed that these species are detected in higher amounts over Rh- than over Pt-based catalysts. These results are in line with higher activity of Rh vs Pt in the SR reaction, i.e. in the formation of CO. Besides a role of the different reactivity of the hydrocarbons (i.e., C_3H_6 vs *n*-heptane) might also be invoked in NCO formation, due to the different chain length (which also causes a different mobility and reactivity toward Steam Reforming reaction, that could occur in those experiments due to the *in situ* produced water) and nature of the chain (i.e., alkane and alkene), as also shown by previous literature data collected over NSR or HC-SCR catalytic systems.[23,24,26,42,49,51]

Notably, during our experiments the presence of CO and NCO species has been observed only upon the reduction of gaseous NO in the presence of oxygen. In this case CO is possibly coming from HC partial oxidation or is due to the occurrence of the SR reaction involving water *in situ* produced by HC oxidation. The so formed CO could thus give rise to a parallel reduction route, involving the intermediacy of NCO. These species are on the other hand not observed when the reduction of gaseous NO is performed in wet conditions likely due to the presence of high amounts of water that (i) involve CO (formed in the SR reaction) in the WGS reaction leading to the formation of CO_2 and H_2 or (ii) readily hydrolyzes isocyanate species to NH_3 and CO_2.[27]

5. CONCLUSIONS

The reduction with *n*-heptane of gaseous NO and NO_x stored over a model $PtBa/Al_2O_3$ catalyst has been investigated by microreactor flow experiments, coupled with the analysis of surface species performed by FT-IR spectroscopy. *n*-Heptane is an effective reductant of both gaseous NO and stored NO_x at temperatures above 200 and 250 °C, respectively. In both cases the reduction leads to the selective formation of N_2 above 300 °C, whereas significant amounts of other species (i.e., N_2O) are also formed at lower temperatures.

Based on the collected data, a reaction pathway for the reduction has been suggested where *n*-heptane initially reduces Pt sites. This leads to the activation/destabilization of the NO_x stored near-by Pt, which are released to the gas phase and/or result in the formation of NO-related intermediates adsorbed over Pt (after the spillover step in the case of NO_x species adsorbed far from Pt). Released NO (or the NO-related intermediates) dissociate over Pt sites into N- and O-adatoms: the O-adatoms are scavenged by the hydrocarbon leading to CO_x and H_2O, whereas N-adatoms may recombine with undissociated NO molecules, with other N-adatoms, or with H-species to give N_2O, N_2, and NH_3, respectively, depending on the Pt oxidation state. Fully reduced Pt sites will favor NO decomposition followed by N−N coupling leading to N_2 (or NH_3 in case in the presence of H-adatoms), while partially reduced Pt will favor the release of unreacted NO and of N_2O. Therefore changes in the Pt oxidation state explain the

selectivity changes observed during the experiments, like evolution of NO and N_2O at low temperatures and almost complete selectivity to N_2 at high temperatures, where *n*-heptane is able to fully reduce Pt. Besides a much higher N_2O formation has been observed in the presence of high NO concentration in the gas phase. In line with the role of the Pt reduction state on the selectivity of the reaction, the presence of O_2 during the runs keeps Pt in a slightly oxidized state particularly at low temperatures thus favoring the formation of N_2O.

Under wet conditions the hydrocarbon molecule is involved in the SR reaction and WGS reactions as well, leading to the formation of H_2 and CO_2. H_2 produced according to these routes participates in the reduction of stored NO_x; nevertheless, the data here presented indicate that the reduction via SR route is not able to account quantitatively for the formation of N_2, due to the poor reactivity of the catalyst in the SR reaction.

According to the pathways previously described, the reduction of the stored NO_x does not involve the participation of isocyanate species whose presence on the other hand has been invoked by other authors. Isocyanate formation is related to the presence of CO in the reduction process, which apparently is not formed in significant amounts under our experimental conditions. When CO has been detected among the reaction products, isocyanates have also been detected, and the reduction pathway involving these species (i.e., reforming of the hydrocarbon to CO followed by reduction of the stored nitrates to isocyanate) proceeds in parallel with the other route and contributes to the reduction of the stored NO_x.

AUTHOR INFORMATION

Corresponding Author

*Phone: +39 02 2399 3272. Fax: +39 02 7063 8173. E-mail: luca.lietti@polimi.it.

Notes

The authors declare no competing financial interest.

REFERENCES

(1) Roy, S.; Baiker, A. *Chem. Rev.* **2009**, *109*, 4054−4091.
(2) Granger, P.; Parvulescu, V. I. *Chem. Rev.* **2011**, *111*, 3155−3207.
(3) Johnson, T. V. *SAE Int. J. Eng.* **2011**, *4*, 143−157.
(4) Takahashi, N.; Shinjoh, H.; Iijima, T.; Suzuki, T.; Yamazaki, K.; Yokota, K.; Suzuki, H.; Miyoshi, N.; Matsumoto, S.; Tanizawa, T.; Tanaka, T.; Tateishi, S.; Kasahara, K. *Catal. Today* **1996**, *27*, 63−69.
(5) Harold, M. P. *Curr. Opin. Chem. Eng.* **2012**, *1*, 303−311.
(6) Epling, W. S.; Campbell, L. E.; Yezerets, A.; Currier, N. W.; Parks, J. E. *Catal. Rev. Sci. Eng.* **2004**, *46*, 163−245.
(7) Nova, I.; Castoldi, L.; Lietti, L.; Tronconi, E.; Forzatti, P.; Prinetto, F.; Ghiotti, G. *J. Catal.* **2004**, *222*, 377−388.
(8) Epling, W. S.; Parks, J. E.; Campbell, G. C.; Yezerets, A.; Currier, N. W.; Campbell, L. E. *Catal. Today* **2004**, *96*, 21−30.
(9) Clayton, R. D.; Harold, M. P.; Balakotaiah, V.; Wan, C. Z. *Appl. Catal., B* **2009**, *90*, 662−676.
(10) Prinetto, F.; Ghiotti, G.; Nova, I.; Castoldi, L.; Lietti, L.; Tronconi, E.; Forzatti, P. *Phys. Chem. Chem. Phys.* **2003**, *5*, 4428−4434.
(11) Xu, J.; Harold, M. P.; Balakotaiah, V. *Appl. Catal., B* **2011**, *104*, 305−315.
(12) Zheng, X.; Kumar, A.; Harold, M. P. *Catal. Today* **2012**, *197*, 66−75.
(13) Lietti, L.; Nova, I.; Forzatti, P. *J. Catal.* **2008**, *257*, 270−282.
(14) Cumaranatunge, L.; Mulla, S. S.; Yezerets, A.; Currier, N. W.; Delgass, W. N.; Ribeiro, F. H. *J. Catal.* **2007**, *246*, 29−34.
(15) Pihl, J. A.; Parks, J. E., II; Daw, C. S.; Root, T. W. *SAE Technol. Pap.* **2006**, 3441.
(16) Forzatti, P.; Lietti, L.; Nova, I.; Morandi, S.; Prinetto, F.; Ghiotti, G. *J. Catal.* **2010**, *274*, 163−175.
(17) Nova, I.; Lietti, L.; Forzatti, P.; Frola, F.; Prinetto, F.; Ghiotti, G. *Top. Catal.* **2009**, *52*, 1757−1761.
(18) Szailer, T.; Kwak, J. H.; Kim, D. H.; Hanson, J. C.; Peden, C. H. F.; Szanyi, J. *J. Catal.* **2006**, *239*, 51−64.
(19) Ji, Y.; Toops, T. J.; Crocker, M. *Appl. Catal., B* **2013**, *140*−*141*, 265−275.
(20) Nova, I.; Castoldi, L.; Lietti, L.; Tronconi, E.; Forzatti, P. *Catal. Today* **2002**, *75*, 431−437.
(21) Poulston, S.; Rajaram, R. R. *Catal. Today* **2003**, *81*, 603−610.
(22) Li, Y. J.; Roth, S.; Dettling, J.; Beutel, T. *Top. Catal.* **2001**, *16*, 139−144.
(23) Abdulhamid, H.; Dawody, J.; Fridell, E.; Skoglundh, M. *J. Catal.* **2006**, *244*, 169−182.
(24) Abdulhamid, H.; Fridell, E.; Skoglundh, M. *Top. Catal.* **2004**, *30*−*1*, 161−168.
(25) Abdulhamid, H.; Fridell, E.; Skoglundh, M. *Appl. Catal., B* **2006**, *62*, 319−328.
(26) Fanson, P. T.; Horton, M. R.; Delgass, W. N.; Lauterbach, J. *Appl. Catal., B* **2003**, *46*, 393−413.
(27) DiGiulio, C. D.; Komvokis, V. G.; Amiridis, M. D. *Catal. Today* **2012**, *184*, 8−19.
(28) Al-Harbi, M.; Radtke, D.; Epling, W. S. *Appl. Catal., B* **2010**, *96*, 524−532.
(29) Miyoshi, N.; Tanizawa, T.; Kasahara, K.; Tateishi, S. *European Patent application* 0 669 157 A1, 1995.
(30) Lindholm, A.; Currier, N. W.; Dawody, J.; Hidayat, A.; Li, J.; Yezerets, A.; Olsson, L. *Appl. Catal., B* **2009**, *88*, 240−248.
(31) Castoldi, L.; Nova, I.; Lietti, L.; Forzatti, P. *Catal. Today* **2004**, *96*, 43−52.
(32) Infantes-Molina, A.; Righini, L.; Castoldi, L.; Loricera, C. V.; Fierro, J. L. G.; Sin, A.; Lietti, L. *Catal. Today* **2012**, *197*, 178−189.
(33) Castoldi, L.; Lietti, L.; Righini, L.; Forzatti, P.; Morandi, S.; Ghiotti, G. *Top. Catal.* **2013**, *56*, 193−200.
(34) Lietti, L.; Daturi, M.; Blasin-Aubé, V.; Ghiotti, G.; Prinetto, F.; Forzatti, P. *ChemCatChem* **2012**, *4*, 55−58.
(35) Morandi, S.; Prinetto, F.; Ghiotti, G.; Castoldi, L.; Lietti, L.; Forzatti, P.; Daturi, M.; Blasin-Aube, V. *Catal. Today* **2014**, *231*, 116−124.
(36) Lavalley, J. C. *Catal. Today* **1996**, *27*, 377−401.
(37) Frola, F.; Prinetto, F.; Ghiotti, G.; Castoldi, L.; Nova, I.; Lietti, L.; Forzatti, P. *Catal. Today* **2007**, *126*, 81−89.
(38) Morandi, S.; Prinetto, F.; Castoldi, L.; Lietti, L.; Forzatti, P.; Ghiotti, G. *Phys. Chem. Chem. Phys.* **2013**, *15*, 13409−13417.
(39) Frola, F.; Manzoli, M.; Prinetto, F.; Ghiotti, G.; Castoldi, L.; Lietti, L. *J. Phys. Chem. C* **2008**, *112*, 12869−12878.
(40) Lietti, L.; Forzatti, P.; Nova, I.; Tronconi, E. *J. Catal.* **2001**, *204*, 175−191.
(41) Kondratenko, V. A.; Baerns, M. *Appl. Catal., B* **2007**, *70*, 111−118.
(42) Lietti, L.; Artioli, N.; Righini, L.; Castoldi, L.; Forzatti, P. *Ind. Eng. Chem. Res.* **2012**, *51*, 7597−7605.
(43) Fridell, E.; Skoglundh, M.; Westerberg, B.; Johansson, S.; Smedler, G. *J. Catal.* **1999**, *183*, 196−209.
(44) Han, P.-H.; Lee, Y.-K.; Han, S.-M.; Rhee, H.-K. *Top. Catal.* **2001**, *16*−*17*, 165−170.
(45) Bisaiji, Y.; Yoshida, K.; Inoue, M.; Umemoto, K.; Fukuma, T. *SAE Technol. Pap.* **2011**, 2089.
(46) Prinetto, F.; Ghiotti, G.; Nova, I.; Lietti, L.; Tronconi, E.; Forzatti, P. *J. Phys. Chem. B* **2001**, *105*, 12732−12745.
(47) Liu, Z.; Anderson, J. A. *J. Catal.* **2004**, *224*, 18−27.
(48) Oh, H.; Luo, J.; Epling, W. S. *Catal. Lett.* **2011**, *141*, 1746−1751.
(49) Oh, H.; Luo, J.; Epling, W. *Top. Catal.* **2013**, *56*, 114−117.
(50) Burch, R.; Breen, J. P.; Meunier, F. C. *Appl. Catal., B* **2002**, *39*, 283−303.
(51) Burch, R.; Sullivan, J. A.; Watling, T. C. *Catal. Today* **1998**, *42*, 13−23.

(52) Burch, R.; Fornasiero, P.; Watling, T. C. *J. Catal.* **1998**, *176*, 204−214.
(53) Burch, R.; Watling, T. C. *Catal. Lett.* **1997**, *43*, 19−23.
(54) Burch, R.; Millington, P. J. *Catal. Today* **1995**, *26*, 185−206.
(55) Captain, D. K.; Amiridis, M. D. *J. Catal.* **1999**, *184*, 377−389.
(56) Captain, D. K.; Amiridis, M. D. *J. Catal.* **2000**, *194*, 222−232.
(57) Okuhara, T.; Hasada, Y.; Misono, M. *Catal. Today* **1997**, *35*, 83−88.
(58) Tanaka, T.; O, T.; Misono, M. *Appl. Catal., B* **1994**, *4*, L1−L9.
(59) Olsson, L.; Fridell, E.; Skoglundh, M.; Andersson, B. *Catal. Today* **2002**, *73*, 263−270.
(60) Inoue, M.; Bisaiji, Y.; Yoshida, K.; Takagi, N.; Fukuma, T. *Top. Catal.* **2013**, *56*, 3−6.
(61) Righini, L.; Castoldi, L.; Lietti, L.; Sauce, S.; Da Costa, P.; Forzatti, P. *Top. Catal.* **2013**, *56*, 1906−1915.